

## Effect of Current Density on Product Distribution for the Electrocatalytic Reduction of CO<sub>2</sub>

Claudio Ampelli<sup>a,\*</sup>, Chiara Genovese<sup>a</sup>, Daniele Cosio<sup>b</sup>, Siglinda Perathoner<sup>a</sup>, Gabriele Centi<sup>b</sup>

<sup>a</sup>Department of Chemical, Biological, Pharmaceutical and Environmental Sciences – University of Messina, ERIC aisbl and CASPE/INSTM, v.le F. Stagno d'Alcontres, 31 – 98166 Messina, Italy

<sup>b</sup>Department of Mathematical, Computer, Physical and Earth Sciences – University of Messina, ERIC aisbl and CASPE/INSTM, v.le F. Stagno d'Alcontres, 31 – 98166 Messina, Italy  
[ampellic@unime.it](mailto:ampellic@unime.it)

The effect of current density on product distribution and yield in the electrochemical reduction of carbon dioxide was studied by processing low-cost and non-critical raw materials. Specifically, the electrodes were prepared by depositing copper (Cu) nanoparticles on functionalized carbon nanotubes (CNTs), then assembled with a gas diffusion layer and a proton exchange membrane. The as-prepared electrodes were fully characterized by different advanced techniques to study their morphological and structural characteristics, as well as their electrochemical properties. Finally, the electrodes were tested in the process of CO<sub>2</sub> electro-reduction by using a compact electrochemical device, designed on purpose to minimize overpotential phenomena. The tests were carried out under a continuous flow of pure CO<sub>2</sub> in 0.1 M KHCO<sub>3</sub> as the electrolyte, applying different voltages (from -0.5 to -1.7 V vs. Ag/AgCl) in order to obtain different current densities (from 0.1 to 2.3 mA cm<sup>-2</sup>, respectively). Furthermore, tests under industrial relevant conditions (high current density) were performed by providing directly 10 mA cm<sup>-2</sup> to the working electrode. Results showed that current density strongly influences the product distribution, with formic acid and CO being the main products at high current density, while products like methanol, ethanol, isopropanol, acetic acid, and oxalic acid were formed at lower applied potential.

### 1. Introduction

The progressive substitution of fossil fuels with renewable energy sources, and in particular with solar energy, requires the need to move to a modified scenario for the industrial chemical production, indicated as solar-driven chemistry (Lanzafame et al., 2017). In this vision, the conversion of CO<sub>2</sub> by electro-reduction process is an attractive and sustainable technology to assist the energy transition and limit greenhouse gas emissions (Rudin et al., 2017). The base concept is that CO<sub>2</sub> and H<sub>2</sub>O can be processed by a direct electrocatalytic route to produce O<sub>2</sub> and more value-added carbon products, through the implementation of an artificial-leaf-type device (Marepally et al., 2017a). In general, many aspects should be taken into account for the realization of an artificial-leaf-type electrocatalytic cell, ranging from the development of the electrocatalytic materials to the design of the cell and the related electrodes, in order to minimize mass and charge transfer and limit overpotential (Ampelli et al., 2017a). The latter factor generally consists of three different types of polarization: 1) the ohmic overpotential, 2) the activation overpotential and 3) the concentration overpotential. The ohmic overpotential refers to the losses caused when ions move through the electrolyte and electrons move through the electrode. The activation overpotential describes the energy needed to overcome the activation energy barrier. The concentration overpotential is related to the mass transfer limitations, i.e. bulk and adsorbed CO<sub>2</sub> diffusion. Except for the concentration overpotential, the other two types of overpotential can be reduced by developing advanced catalytic materials designed on purpose in order to minimize the resistances due to Helmholtz double layers (Qiao et al., 2016). For lowering the concentration overpotential, instead, studies on controlling operational conditions (i.e. electrolyte, pressure, current density, cell configuration) should be

performed (Lobaccaro et al., 2016). Moreover, varying one of these conditions may also influence the product distribution. The main products obtained by CO<sub>2</sub> electrochemical reduction are formic acid (or formate) and carbon monoxide, as well as hydrogen produced by the side reaction of water splitting. In addition, more value added products can be produced but only in small amounts. For example, Kuhl et al. (2012) observed a total of 16 different products, by processing CO<sub>2</sub> on metallic copper surface, including aldehydes, ketones, alcohols and carboxylic acids in the range C1-C3. The selective distribution of CO<sub>2</sub> products mainly depends on the nature of the electrocatalyst, but the selectivity is also strongly influenced by the current density. For industrial application, in which high space-time yields are mandatory, high current densities are often required, for reasons related to stoichiometry and economics (Oloman and Li, 2008). Thus, the products may be greatly different by changing the current density and this should be considered in scale-up industrial operation. In this context, the main objective of this work is to show the dependence of product distribution on current density, through the analysis of CO<sub>2</sub> electro-reduction over carbon nanotubes doped with copper nanoparticles. Carbon nanotubes were chosen for their high conductivity, mechanical resistance and stability. Moreover, carbon nanotubes can easily be modified by introducing oxygen functional groups to anchor the metal nanoparticles (i.e. Cu). The electrocatalysts were synthesised by wet impregnation and deposited/assembled with a gas diffusion layer and a proton exchange membrane to obtain a Membrane Electrode Assembly - MEA (in analogy with fuel cells). Then, the electrodes were tested in the electrocatalytic reduction of CO<sub>2</sub> by processing pure CO<sub>2</sub> in KHCO<sub>3</sub> aqueous electrolyte under different applied potentials.

## 2. Experimental

### 2.1 Synthesis and characterization

Copper nanoparticles (Cu NPs) were deposited on pre-functionalized carbon nanotubes (CNTs, PR-24-XT-PS Pyrograf®) by an incipient wetness impregnation method using an aqueous solution of ethanol containing the copper salt precursor Cu(NO<sub>3</sub>)<sub>2</sub>·3H<sub>2</sub>O. After drying at 60 °C for 24 h, the samples were annealed for 2 h at 350 °C and reduced at 400 °C under a slow H<sub>2</sub> flow. The total amount of Cu loaded onto the CNTs was 5 wt.%. The as-prepared Cu NPs-CNTs were then deposited on a gas diffusion layer (GDL, GDL29BC Sigracet®) using a similar impregnation method in anhydrous ethanol. The quantity of Cu NPs-CNTs was chosen in order to obtain a final Cu loading of 0.1 mg cm<sup>-2</sup> (per geometrical area of GDL). Details about the preparation of the electrodes were earlier reported (Marepally et al., 2017b). The electrodes were then fully characterized by X-Ray Diffraction (XRD) and Transmission Electron Microscopy (TEM) to study their morphological and structural characteristics, as well as by Linear Sweep Voltammetry (LSV) and Cyclic Voltammetry (CV) to evaluate their electrochemical properties.

### 2.2 Testing

Cu NPs-CNTs/GDL electrodes were tested in the process of CO<sub>2</sub> electrocatalytic reduction. The electrochemical device was made of transparent material (Plexiglas®) to allow an internal visual inspection, working in a three-electrode configuration: 1) working electrode (Cu NPs-CNTs/GDL), 2) counter-electrode (Pt rod) and 3) reference electrode (Ag/AgCl). A Nafion® membrane (N115, supplied by Ion Power) was used to separate the two half-cells. Both the compartments (cathode and anode) were filled with 0.1 M KHCO<sub>3</sub> as the electrolyte under a continuous flow of pure CO<sub>2</sub> (20 mL min<sup>-1</sup>) to saturate the aqueous solutions and operate under the same pH (about 7.5-8.0) in both the half-cells, at least at the initial stage of testing. The active electrocatalytic area was about 5 cm<sup>2</sup>. Figure 1 shows a scheme of the electrochemical device (Ampelli et al., 2015).

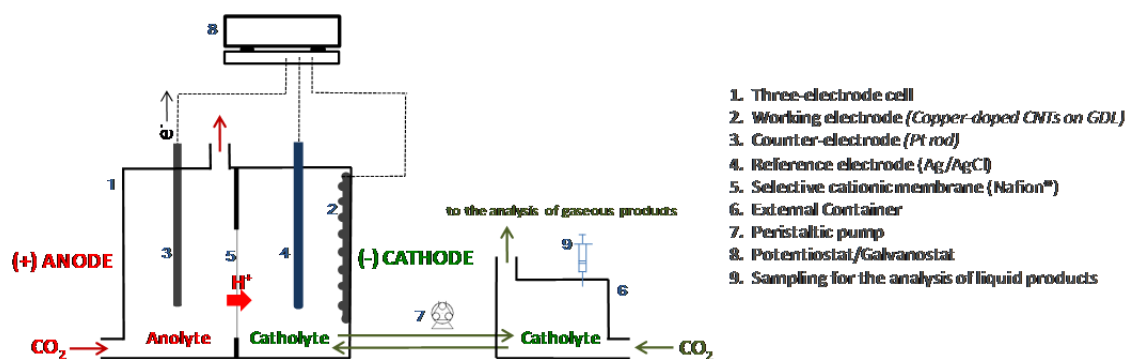


Figure 1: Schematic representation of the electrochemical cell. Adapted from Ampelli et al. (2015).

The tests were carried out at different applied potentials (from -0.5 to -1.7 V vs. Ag/AgCl), corresponding to different current densities (from 0.1 to 2.3 mA cm<sup>-2</sup>, respectively). A further test was carried out in amperometric mode applying directly 10 mA cm<sup>-2</sup>, in order to evaluate the catalytic performance under industrial relevant conditions.

The gas products (H<sub>2</sub>, CO) were analysed by using a micro Gas Chromatograph (microGC Pollution Srl) equipped with two modules and TCD as the detectors. The liquid products were analysed by using a Gas Chromatograph-Mass Spectrometer (GC-MS Thermo 1310-Tsq 8000 Evo, column Stabilwax) and Ion Chromatography (IC Metrohm 940 Professional, column Metrohm Organic Acids).

### 3. Results and discussion

#### 3.1 Morphological and electronic characterization

Figure 2 shows the XRD pattern of Cu NPs-CNTs. The dominant diffraction peak at 26.4° can be assigned to the (002) planes of the hexagonal graphite structure of CNTs with an interplanar spacing of 0.34 nm. Two twin peaks at 2θ = 35.67° and 38.90° and a weaker peak at 2θ = 48.97° are observed, corresponding to the planes (020), (111) and (202) of monoclinic CuO, respectively (JCPDS 80-1916). The average crystallite size can be determined by the Scherrer equation (Holzwarth and Gibson, 2011) and it is in the range of 38-40 nm.

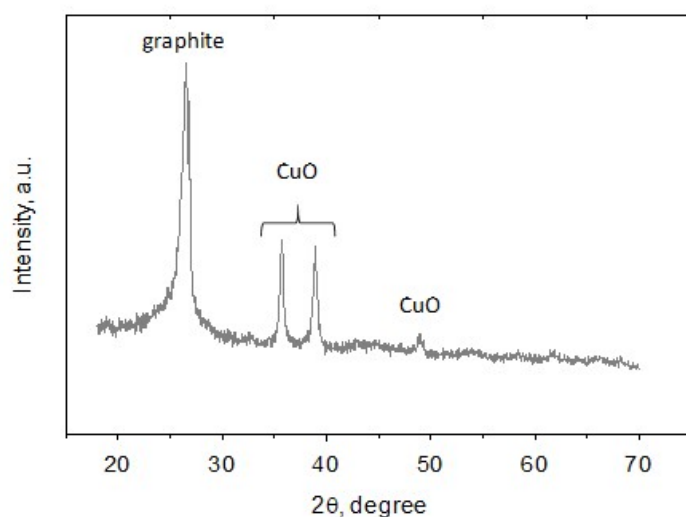


Figure 2: XRD pattern of CuNPs-CNTs.

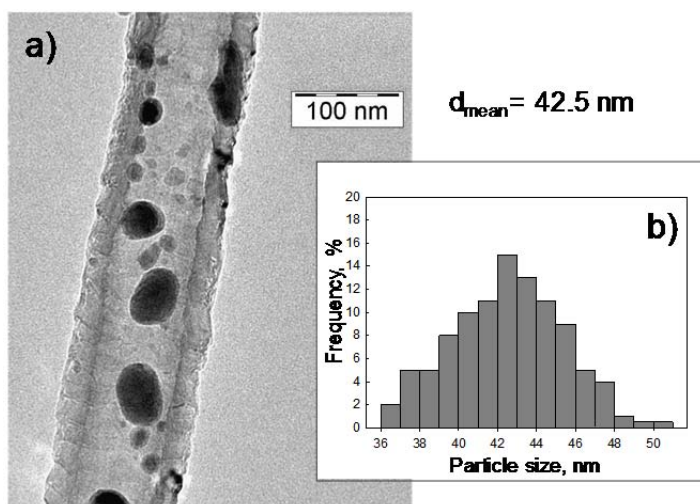


Figure 3: a) TEM image of CuNPs-CNTs and b) particle size distribution.

The morphology and the particle size distribution of Cu NPs-CNTs were determined by Transmission Electron Microscopy (TEM). Figure 3a shows a representative TEM image of a Cu-doped carbon nanotube, evidencing round-like Cu particles mainly localized inside the nanotube with a relatively narrow size distribution (see Figure 3b). The estimated average particle diameter is 42.5 nm ( $\pm$  3.5 nm), which is in good agreement with XRD results.

### 3.2 Electrocatalytic tests

Despite the many kinds of electrocatalysts investigated in literature, copper is the only one that exhibits appreciable activity and Faradaic efficiency for reducing CO<sub>2</sub> to hydrocarbons and oxygenates (Kuhl et al. 2014). The use of Cu NPs deposited onto nanocarbons (i.e. CNTs) with respect to a Cu foil, may improve the catalytic activity and facilitate the formation of C-C bond, due to the positive catalytic effect of the interface between Cu NPs and CNTs (Genovese et al., 2017).

Table 1 reports the different kinds of carbon products obtained in the electrocatalytic tests of CO<sub>2</sub> reduction over Cu NPs-CNTs/GDL. They range from C1 products (CO, formic acid and methanol) to C2-C3 products (ethanol, acetic acid, oxalic acid and isopropanol).

Table 1: Carbon products obtained in CO<sub>2</sub> electrocatalytic reduction

C1	C2	C3
Carbon monoxide	Ethanol	Isopropanol
Formic acid	Acetic acid	
Methanol	Oxalic acid	

Both the product distribution and yield strongly depend on the current density and applied potential. Figure 4 shows the profiles of production rate versus current density. All the points in the graph have been obtained by calculating the average production rates from three different tests (standard deviation less than 5 %).

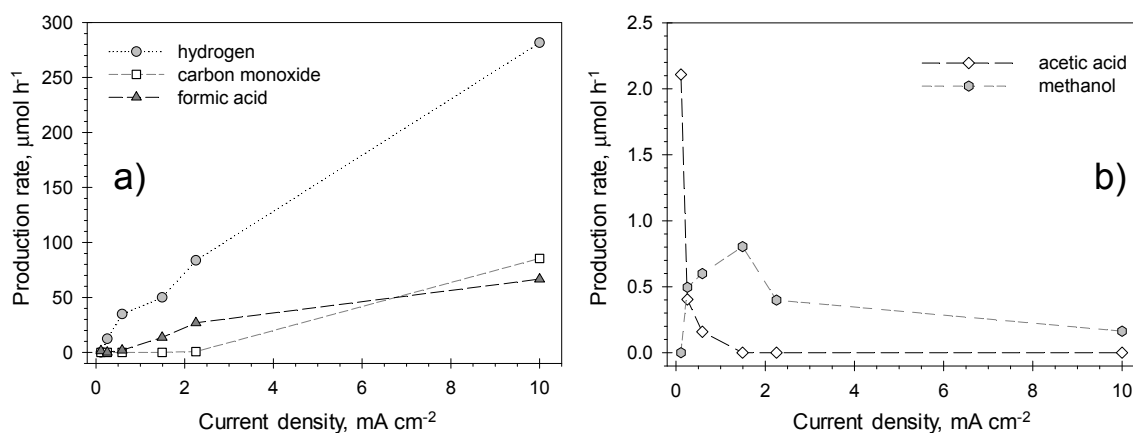


Figure 4: Production rate vs. current density for a) H<sub>2</sub>, CO and formic acid and b) methanol and acetic acid.

Formic acid and CO were the carbon products formed with the highest yield, especially at high current density (see Figure 4a). Hydrogen evolution rate was also high and increased regularly with the current density, with a slight slowdown at 1.5  $\text{mA cm}^{-2}$ . At the same current density, the methanol production rate reached a maximum, while the formation of acetic acid decreased with the current density (see Figure 4b). Furthermore, Faradaic Efficiency (FE) was calculated by taking into account the number of electrons needed to form each reduction product from CO<sub>2</sub> with respect to the provided electric current (Ampelli et al., 2017b). Figure 5 shows the product distribution expressed in terms of FE %. All the values reported in Figures 4 and 5 refer to averages from three different tests (the calculated standard deviation is lower than 5 %).

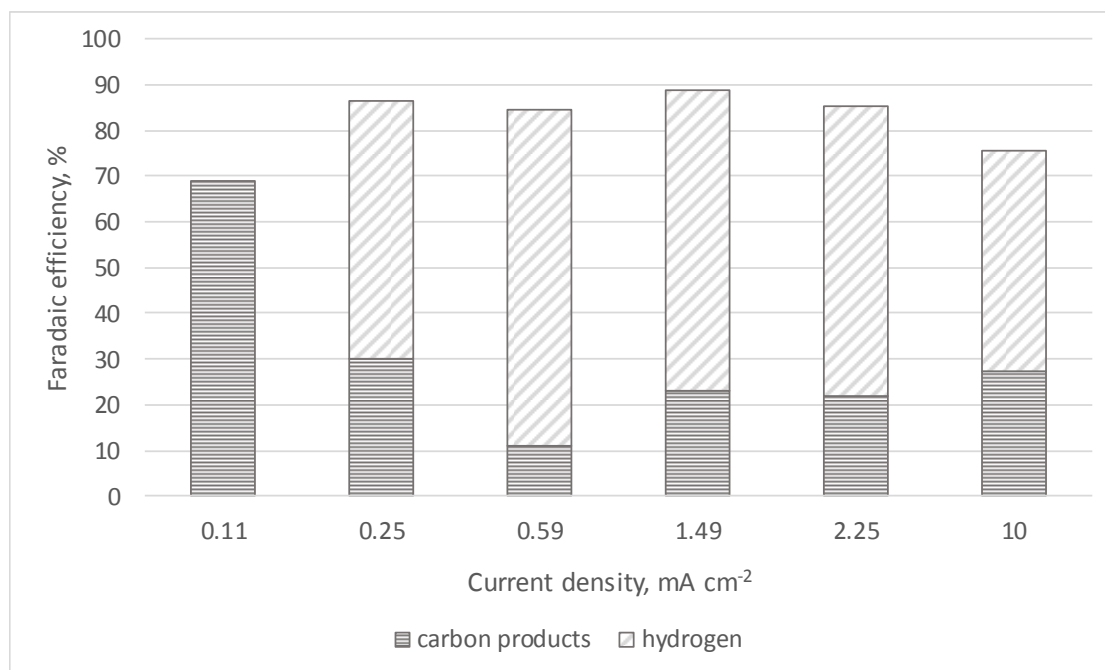


Figure 5: Faradaic efficiency (%) vs. current density.

As it can be observed, the total Faradaic Efficiency values are all ranging from 75 to almost 90 %, except when the current density is very low (0.11 mA cm<sup>-2</sup>). At this current density, no hydrogen was detected, as the applied voltage (-0.5 V vs. Ag/AgCl) was not sufficient to activate water reduction. However, under industrial relevant conditions (10 mA cm<sup>-2</sup>), the carbon Faradaic selectivity was quite high (27.4 %), indicating Cu NPs-CNTs/GDL as a promising electrocatalyst for CO<sub>2</sub> reduction process. The values of FE for all the products have been summarized in Table 2, confirming that formic acid was the main carbon product formed, while carbon monoxide started to form at 2.25 mA cm<sup>-2</sup> and became even higher than formic acid at 10 mA cm<sup>-2</sup>. However, at low current density the product distribution is quite different: methanol, ethanol and isopropanol (especially at 0.25 mA cm<sup>-2</sup>, corresponding to -1.0 V vs. Ag/AgCl) were formed, while acetic acid and oxalic acid were produced at -0.5 V vs. Ag/AgCl (0.11 mA cm<sup>-2</sup>). These are examples of products involving C-C bond formation (Genovese et al., 2013).

Table 2: Faradaic Efficiency (FE) for all the CO<sub>2</sub> reduction products at different current densities

Current density, mA cm <sup>-2</sup>	Faradaic Efficiency (%)					
	0.11	0.25	0.59	1.49	2.25	10.0
Carbon monoxide	-	-	-	-	0.57	14.7
Formic acid	7.9	0.26	3.9	16.5	19.7	11.4
Methanol	-	5.5	3.7	2.9	0.88	0.08
Ethanol	8.0	2.9	0.57	2.0	0.25	0.26
Acetic acid	47.4	6.0	1.3	-	-	-
Oxalic acid	4.1	0.37	1.4	0.04	0.34	0.70
Isopropanol	1.64	14.9	0.38	1.85	-	0.22
Total carbon	69.0	29.9	11.3	23.3	21.7	27.4
Hydrogen	-	56.4	73.2	65.6	63.5	48.3
Total products	69.0	86.3	84.5	88.9	85.2	75.7

#### 4. Conclusions

This contribution focused on the preparation of efficient electrodes to be implemented in a compact electrocatalytic reactor for the production of value-added chemicals. Particularly, copper-doped carbon nanotubes were synthesised and deposited/assembled with a gas diffusion layer and a proton exchange membrane to form a Membrane Electrode Assembly. Testing these electrodes in CO<sub>2</sub> electrocatalytic reduction under different applied voltages showed that the current density strongly affects the product

distribution. Specifically, acetic acid, ethanol, formic acid, oxalic acid, methanol, and isopropanol were the main products obtained at lower current density, while the production of formic acid, CO and H<sub>2</sub> increased at higher current density, evidencing a direct influence of this parameter on C-C bond formation. When tested under industrial relevant conditions (i.e. high current density), the copper-based electrodes provided a relatively high Faradaic efficiency (27.4 %), opening the route towards a practical implementation of CO<sub>2</sub> electroreduction process with low-cost and earth abundant materials as electrocatalysts. However, further studies are needed to improve the catalytic performance by both catalyst and cell design.

### Acknowledgments

This work was funded by the European Union through the A-LEAF project (732840-A-LEAF), which is gratefully acknowledged.

### References

- Ampelli C., Genovese C., Tavella F., Perathoner S., Centi G., 2017a, Nano-engineered electrodes for the generation of solar fuels: Benefits and drawbacks of adopting a photo-electrocatalytic (PECa) approach, *Chemical Engineering Transactions*, 57, 1597–1602.
- Ampelli C., Tavella F., Perathoner S., Centi G., 2017b, Engineering of photoanodes based on ordered TiO<sub>2</sub>-nanotube arrays in solar photo-electrocatalytic (PECa) cells, *Chemical Engineering Journal*, 320, 352–362.
- Ampelli C., Genovese C., Errahali M., Gatti G., Marchese L., Perathoner S., Centi G., 2015, CO<sub>2</sub> capture and reduction to liquid fuels in a novel electrochemical setup by using metal-doped conjugated microporous polymers, *Journal of Applied Electrochemistry*, 45, 701–713.
- Genovese C., Ampelli C., Perathoner S., Centi G., 2017, Mechanism of C-C bond formation in the electrocatalytic reduction of CO<sub>2</sub> to acetic acid. A challenging reaction to harvest renewable energy with chemistry, *Green Chemistry*, 19, 2406–2415.
- Genovese C., Ampelli C., Perathoner S., Centi G., 2013, A Gas-phase Electrochemical Reactor for Carbon Dioxide Reduction back to Liquid Fuels, *Chemical Engineering Transactions*, 32, 289–294.
- Holzwarth U., Gibson N., 2011, The Scherrer equation versus the 'Debye-Scherrer equation', *Nature Nanotechnology*, 6, 534.
- Kuhl K.P., Hatsukade T., Cave E.R., Abram D.N., Kibsgaard, J., Jaramillo T.F., 2014, Electrocatalytic Conversion of Carbon Dioxide to Methane and Methanol on Transition Metal Surfaces, *Journal of the American Chemical Society*, 136, 14107–14113.
- Kuhl K.P., Cave E.R., Abram D.N., Jaramillo T.F., 2012, New insights into the electrochemical reduction of carbon dioxide on metallic copper surfaces, *Energy & Environmental Science*, 2012, 5, 7050–7059.
- Lanzafame P., Abate S., Ampelli C., Genovese C., Passalacqua R., Centi G., Perathoner S., 2017, Beyond Solar Fuels: Renewable Energy-Driven Chemistry, *ChemSusChem*, 10, 4409–4419.
- Lobaccaro P., Singh M.R., Lee Clark E., Kwon Y., Bell A.T., Ager J.W., 2016, Effects of temperature and gas-liquid mass transfer on the operation of small electrochemical cells for the quantitative evaluation of CO<sub>2</sub> reduction electrocatalysts, *Physical Chemistry Chemical Physics*, 18, 26777–26785.
- Marepally B.C., Ampelli C., Genovese C., Saboo T., Perathoner S., Wisser F.M., Veyre L., Canivet J., Quadrelli E.A., Centi G., 2017a, Enhanced formation of >C1 Products in the Electroreduction of CO<sub>2</sub> by Adding a CO<sub>2</sub> Adsorption Component to a Gas-Diffusion Layer-Type Catalytic Electrode, *ChemSusChem*, 10, 4442–4446.
- Marepally B.C., Ampelli C., Genovese C., Tavella F., Veyre L., Thieuleux C., Quadrelli E.A., Perathoner S., Centi G., 2017b, Role of small Cu nanoparticles in the behaviour of nanocarbon-based electrodes for the electrocatalytic reduction of CO<sub>2</sub>, *Journal of CO<sub>2</sub> Utilization*, 21, 534–542.
- Oloman C., Li H., 2008, Electrochemical Processing of Carbon Dioxide, *ChemSusChem*, 1, 385–391.
- Qiao J., Liu Y., Zhang J., 2016, Eds. *Electrochemical Reduction of Carbon Dioxide: Fundamentals and Technologies*, 1st ed.; CRC Press, Boca Raton, USA.
- Rudin S.N.F.M., Muis Z., Hashim H., Ho W.S., 2017, Overview of carbon reduction, capture, utilization and storage: Development of new framework, *Chemical Engineering Transactions*, 56, 649–654.